




6-2015

Suspension model for blood flow through a tapering catheterized inclined artery with asymmetric stenosis

Devajyoti Biswas
Assam University

Moumita Paul
Assam University

Follow this and additional works at: <https://digitalcommons.pvamu.edu/aam>

 Part of the [Biology Commons](#), [Fluid Dynamics Commons](#), and the [Other Physical Sciences and Mathematics Commons](#)

Recommended Citation

Biswas, Devajyoti and Paul, Moumita (2015). Suspension model for blood flow through a tapering catheterized inclined artery with asymmetric stenosis, *Applications and Applied Mathematics: An International Journal (AAM)*, Vol. 10, Iss. 1, Article 28.

Available at: <https://digitalcommons.pvamu.edu/aam/vol10/iss1/28>

This Article is brought to you for free and open access by Digital Commons @PVAMU. It has been accepted for inclusion in *Applications and Applied Mathematics: An International Journal (AAM)* by an authorized editor of Digital Commons @PVAMU. For more information, please contact hvkoshy@pvamu.edu.



Suspension model for blood flow through a tapering catheterized inclined artery with asymmetric stenosis

Devajyoti Biswas and Moumita Paul*

Department of Mathematics
Assam University
Silchar: 788011, India
mpmaths@gmail.com

*Corresponding author

Received: March 27, 2013; Accepted: April 7, 2015

Abstract

We intend to study a particle fluid suspension model for blood flow through an axially asymmetric but radially symmetric mild stenosis in the annular region of an inclined tapered artery and a co-axial catheter in a suitable flow geometry has been considered to investigate the influence of velocity slip at the stenotic wall as well as hematocrit, shape parameter. The model also includes the tapering effect and inclination of the artery. Expressions for the flow variables have been derived analytically and their variations with various flow parameters are represented graphically. The results for the different values of the parameters involved show that the impedance to flow increases with stenosis height, hematocrit and catheter radius. However, it decreases with the shape parameter, angle of inclination of artery and velocity slip at the stenotic wall. The present analysis is an extension of the work by Chakraborty et al. (2011) and also includes several theoretical models of arterial stenosis in the uniform, tapering and catheterized tubes, with the consideration of velocity slip or zero slip at the vessel wall. Finally, some biological implications of this theoretical modeling are included in brief.

Keywords: Blood; hematocrit; catheter; impedance; shear stress; stenosis; slip; taper angle

MSC 2010 No.: 76Z05, 92C10

1. Introduction

Atherosclerosis (stenosis) is a wide spread Cardiovascular (CVS) disease. Majority of deaths in developed countries result from CVS diseases and most of which are associated with abnormal flow in arteries (Ku, 1997). Stenosis is an abnormal and unnatural growth that develops at one or more locations of Cardiovascular System, under diseased conditions and causes serious circulatory disorders (Guyton, 1970; Young, 1968). There is no exact

information regarding such unfamiliar growth at an arterial wall. However, due to the deposits of atherosclerotic plaques, cholesterol, lipids, fats etc., at an innermost arterial wall, the kind of formation may develop at the vessel wall.

It is reported that circulatory disorders could be responsible for over seventy five percent of all deaths (Srivastava et al. 2010). These circulatory disorders may include (i) the narrowing in body passage or orifice, leading to the reduction in nutrient supply an impediment to blood flow in constricted artery regions, (ii) blockage of artery, in turning the flow irregular and causing abnormality of blood flow and (iii) presence of stenosis at one or more major blood vessels, supplying blood to heart or brain could lead to various arterial and Cardiovascular diseases like, angina pectoris, myocardial infarction, cerebral accident, coronary thrombosis, heart attack, strokes, thrombosis etc. (Young, 1968). In view of the above, blood flow modeling in arterial system is a topic of recent interest to theoretical and clinical investigators.

Blood is a suspension of different cells or corpuscles in plasma. Most of the models on blood flow have dealt with a one phase model (Womersley, 1955; Lightfoot, 1974; Sud and Sekhon, 1985; Young, 1968). As blood is a suspension, a two phase model seems to be more appropriate. At low shear rates and while flowing in narrow channels, blood behaves as a non-Newtonian fluid (Merril and Pelletier, 1967; Charm and Kurland, 1974). The theoretical results of Haynes (1960) indicate that blood cannot be considered as a single phase homogeneous viscous fluid while flowing through narrow arteries (of diameter $\leq 1000\mu\text{m}$). Srivastava and Srivastava (1983) have mentioned that blood can be suitably represented by a macroscopic two-phase model (i.e., a suspension of red cells in plasma) in small vessels (of diameter $\leq 2400\mu\text{m}$). Recently, Chakraborty et al. (2011) have considered a two-phase model for blood flow through a constricted artery.

In most of the aforementioned works, blood vessels are considered horizontal. It is well known that many ducts in the human physiological systems are not horizontal, rather they have some inclination to the axis. The force of gravity comes into the flow field due to the consideration as an inclined tube. Steady blood flow through an inclined non-uniform tube with multiple stenoses has been proposed by Maruti Prasad and Radhakrishnachandramacharya (2008). Chakraborty et al. (2011) have proposed a blood flow model through an inclined tube with stenosis.

Normally, in circulatory systems arteries are assumed to be clear pipes and blood can flow easily without any hindrance and performs specific functions like, transporting nutrients, maintaining metabolic processes and regulating body balance (Guyton, 1970). The study of circulatory systems is pretty old and the quest for knowing the living world, especially the human physiological systems had its beginning in the long past (Fung, 1981). In fact, both Aristotle and Leonardo the Vinci were interested in blood flow through human circulatory systems. Many investigators have proposed theoretical models on blood flow from various considerations (Fung, 1981). Blood flow through stenosed arteries with axially symmetric stenosis, have been proposed by many researchers (Young, 1968; MacDonald, 1979). Flow of blood in obstructed arteries with axially non-symmetrical stenosis is investigated by Mekheimer and Kothari (2010), Chakraborty et al. (2011). Pressure-flow relationship alters the blood flow in a stenosed artery. Sometimes, for some clinical purposes, catheters are inserted in arteries. The pressure-flow relationship changes appreciably when a catheter is inserted in a stenosed artery. Blood flow models through catheterized stenosed artery have been proposed by Mekheimer and Kothari (2010), Chakraborty et al. (2011).

In human systems, there prevail different geometries in blood vessels such as, circular, branched, bifurcated, tapered, inclined etc. (Guyton, 1970). It could be important to

investigate blood flow through an inclined tapered artery for Newtonian fluid (Biswas and Paul, 2012) and for the two phase flow, in the present study.

Recently, Chakraborty et al. (2011) have used the slip condition in their two-phase stenosed, but to the authors knowledge, no theoretical or experimental work has been done to analyze the effects of velocity slip at the stenotic wall on macroscopic two-phase (plasma red-cell) blood flow model, in an inclined constricted catheterized tapering artery.

In the present analysis, an effort has been made to study the effects of velocity slip (at the stenotic vessel wall), hematocrit, tapering tube, catheterization and inclination of the artery on the flow variables for annular blood flow through an inclined, catheterized tapering artery with the formation of an axially asymmetric mild stenosis, by considering blood to behave as a particle-fluid suspension.

2. Mathematical Formulation:

We consider a steady, laminar and fully developed flow of blood (supposed to be incompressible) through the annular region of an inclined tapering circular tube and a co-axial rigid catheter, with the formation of an axially asymmetric mild stenosis. The flow geometry of the inclined catheterized tapering vessel and the non-axisymmetrical stenosis but radially symmetric growth, are presented in Figure 1 and 2 respectively.

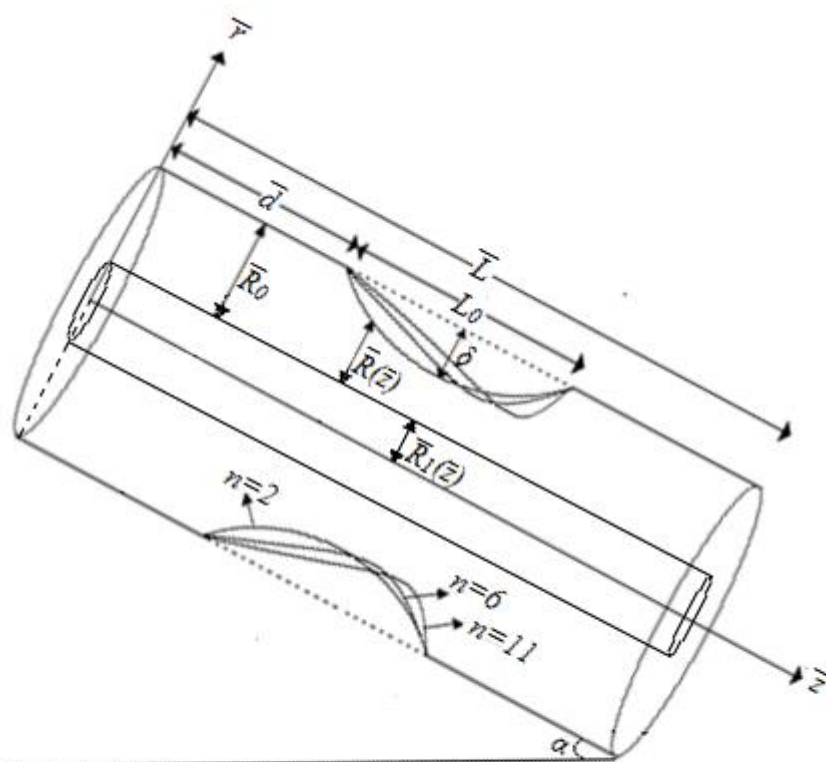


Figure 1. Geometry of an inclined stenosed artery with axially non-symmetrical stenosis

The geometry of an arterial asymmetric stenosis, developed along a tapered wall, can be reproduced (Mekheimer and Kothari, 2008) as

$$\bar{R}(\bar{z}) = b(\bar{z})[1 - \bar{A}(\bar{L}_0^{n-1}(\bar{z} - \bar{d}) - (\bar{z} - \bar{d})^n)], \bar{d} \leq \bar{z} \leq \bar{d} + \bar{L}_0,$$

$$= b(\bar{z}), \quad \text{otherwise,} \quad (1)$$

with

$$b(\bar{z}) = \bar{R}_0 + \xi(\bar{z}),$$

where $b(\bar{z})$ represents the radius of the tapered arterial segment along the stenotic portion, $\xi(=\tan\Phi)$ is the tapering parameter, Φ the tapering angle, $\bar{R}(\bar{z})$ is the radius of the stenosed region, \bar{R}_0 is the radius of the artery in the non-stenotic region, \bar{R}_1 is the catheter radius,

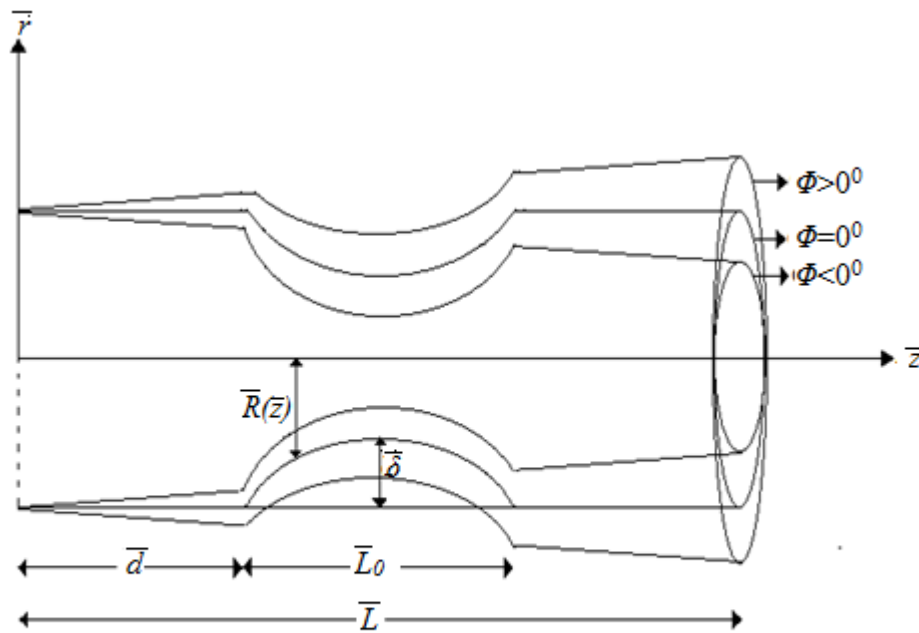


Fig. 2. Geometry of the stenosed tapered artery for different taper angle

$n(\geq 2)$ is a parameter (treated as shape parameter), signifying the stenosis shape which includes the symmetric stenosis case when $n=2$, and, (r, z) are the radial and axial coordinates, the respective quantities \bar{L}_0 , \bar{d} and \bar{L} denote the stenosis length, its location and the total length of the obstructed artery. The parameter \bar{A} is taken as

$$\bar{A} = \frac{\bar{\delta} n^{n/(n-1)}}{\bar{R}_0 \bar{L}_0^n (n-1)}, \quad (2)$$

where $\bar{\delta}$ is the maximum height of the stenosis at a distance $\bar{z} = \bar{d} + \frac{\bar{L}_0}{n^{1/(n-1)}}$.

The body fluid blood is assumed to behave like a two fluid model that is a mixture of erythrocytes and plasma. The equations describing the steady flow of a two phase model, comprising the fluid phase and particle phase of blood may be expressed as (Srivastava and Srivastava, 1983) as

$$(1-C)\bar{\rho}_f(\bar{v}_f \frac{\partial}{\partial r} + \bar{u}_f \frac{\partial}{\partial z})\bar{v}_f = -(1-C)\frac{\partial \bar{p}}{\partial r} \\ + (1-C)\bar{\mu}_s(C)(\frac{\partial^2}{\partial r^2} + \frac{\partial^2}{\partial z^2} + \frac{1}{r}\frac{\partial}{\partial r} - \frac{1}{r})\bar{v}_f + C\bar{S}(\bar{v}_p - \bar{v}_f) - (1-C)\bar{\rho}_f \bar{g} \cos \alpha, \quad (3)$$

$$(1-C)\bar{\rho}_f(\bar{v}_f \frac{\partial}{\partial r} + \bar{u}_f \frac{\partial}{\partial z})\bar{u}_f = -(1-C)\frac{\partial \bar{p}}{\partial z} \\ + (1-C)\bar{\mu}_s(C)(\frac{\partial^2}{\partial r^2} + \frac{\partial^2}{\partial z^2} + \frac{1}{r}\frac{\partial}{\partial r})\bar{u}_f + C\bar{S}(\bar{u}_p - \bar{u}_f) + (1-C)\bar{\rho}_f \bar{g} \sin \alpha, \quad (4)$$

$$\frac{\partial}{\partial r}(1-C)\bar{v}_f + \frac{\partial}{\partial z}(1-C)\bar{u}_f + \frac{1}{r}(1-C)\bar{v}_f = 0. \quad (5)$$

Particulate phase:

$$C\bar{\rho}_p(\bar{v}_p \frac{\partial}{\partial r} + \bar{u}_p \frac{\partial}{\partial z})\bar{v}_p = -C\frac{\partial \bar{p}}{\partial r} + C\bar{S}(\bar{v}_f - \bar{v}_p) - C\bar{\rho}_p \bar{g} \cos \alpha, \quad (6)$$

$$C\bar{\rho}_p(\bar{v}_p \frac{\partial}{\partial r} + \bar{u}_p \frac{\partial}{\partial z})\bar{u}_p = -C\frac{\partial \bar{p}}{\partial z} + C\bar{S}(\bar{u}_f - \bar{u}_p) + C\bar{\rho}_p \bar{g} \sin \alpha, \quad (7)$$

$$\frac{\partial}{\partial r}(C\bar{v}_p) + \frac{\partial}{\partial z}(C\bar{u}_p) + \frac{1}{r}(C\bar{v}_p) = 0, \quad (8)$$

where (\bar{r}, \bar{z}) are (radial, axial) coordinates, (\bar{u}_f, \bar{u}_p) and (\bar{v}_f, \bar{v}_p) are the respective axial and radial velocities of fluid and particle phases, $(\bar{\rho}_f, \bar{\rho}_p)$ are corresponding densities of two stages, $\bar{\mu}_s \cong \bar{\mu}_s(C)$ is the suspension viscosity, C denotes the constant volume fraction density of the particles (called hematocrit), \bar{p} is the pressure, \bar{S} is the drag coefficient of interaction between these two (fluid, particle) phases, \bar{g} is the acceleration due to gravity and α is the inclination of the tube to the horizontal. The expression for the drag coefficient of interaction \bar{S} and empirical relation for the viscosity of suspension $\bar{\mu}_s$, may be taken (Srivastava, 1995; 2002) as

$$\bar{S} = \frac{9}{2} \frac{\bar{\mu}_0}{\bar{a}_0^2} \frac{[4 + 3(8C - 3C^2)^{1/2} + 3C]}{(2 - 3C)^2}, \quad (9)$$

$$\bar{\mu}_s = \frac{\bar{\mu}_0}{1 - qC}, \quad (10)$$

$$q = 0.07 \exp[2.49C + \frac{1107^0 K}{T} \exp(-1.69C)], \quad (11)$$

where \bar{a}_0 is the particle radius, $\bar{\mu}_0$ is the plasma viscosity and T is measured in absolute temperature.

We introduce the following dimensionless quantities in the foregoing analysis:

$$z = \frac{\bar{z}}{R_0}, d = \frac{\bar{d}}{R_0}, r = \frac{\bar{r}}{R_0}, R = \frac{\bar{R}}{R_0}, \delta = \frac{\bar{\delta}}{R_0}, \mu = \frac{\bar{\mu}}{\mu_0}, \frac{dp}{dz} = \frac{\frac{d\bar{p}}{d\bar{z}}}{q_0}, \bar{S} = \frac{S}{\mu_0 / R_0^2},$$

$$A = \frac{\bar{A} \bar{R}_0^n}{\bar{U}_0}, (u_f, u_p) = \frac{(\bar{u}_f, \bar{u}_p)}{\bar{U}_0}, (L, L_0) = (\bar{L}, \bar{L}_0) / \bar{R}_0, F = \frac{\bar{q}_0}{(4(1-C)\bar{\rho}_f g)},$$

$$G = \frac{\bar{q}_0}{(4C\bar{\rho}_p g)}, \bar{U}_0 = \frac{\bar{q}_0 \bar{R}_0^2}{4\mu_0},$$
(12)

where \bar{U}_0 is the maximum velocity at the axis of a horizontal tube with radius \bar{R}_0 and \bar{q}_0 is the negative of the pressure gradient, in case of an unobstructed uniform horizontal tube.

Due to the non-linearity of the convective acceleration terms, integration of equations (3-8) is a difficult task. It is already reported by many investigators (Srivastava, 1995, 2002; Sankar and Lee, 2009) that the radial velocity being very small for the case of a mild stenosis ($\bar{\delta} / \bar{R}_0 \ll 1$), subject to additional conditions

$$\text{Re}(\bar{\delta} n^{n-1} / \bar{L}_0) \ll 1 \text{ and } n^{n-1} \bar{R}_0 / \bar{L}_0 \sim O(1),$$

can be neglected.

In view of the above simplified form of above partial equations (3)-(8), governing the steady flow of a particulate (particle- fluid) suspension with the above parameters, can be expressed in the following coupled equations

$$(1-C) \frac{d\bar{p}}{d\bar{z}} = (1-C) \frac{\bar{\mu}_s(C)}{r} \frac{\partial}{\partial r} \left(r \frac{\partial \bar{u}_f}{\partial r} \right) + C\bar{S}(\bar{u}_p - \bar{u}_f) + (1-C)\bar{\rho}_f \bar{g} \sin \alpha,$$
(13)

$$C \frac{d\bar{p}}{d\bar{z}} = C\bar{S}(\bar{u}_f - \bar{u}_p) + C\bar{\rho}_p \bar{g} \sin \alpha,$$
(14)

In integrating equations (13-14), boundary conditions employed are the following:

$$\bar{u}_f = \bar{u}_s \quad \text{at} \quad \bar{r} = \bar{R},$$
(15)

$$\bar{u}_f = 0, \bar{u}_p = \text{finite} \quad \text{at} \quad \bar{r} = \bar{R}_1,$$
(16)

where \bar{u}_s is the slip velocity at the tapered constricted wall (Biswas and Chakraborty, 2009). Using the non-dimensional quantities as included in equation (12), the following equations have been obtained in dimensionless form.

The flow geometry expressed in equation (1) can be written as

$$R = (1 + \xi z)[1 - A(L_0^{n-1}(z-d) - (z-d)^n)], d \leq z \leq d + L_0,$$

$$= (1 + \xi z), \text{ otherwise.}$$
(17)

The equations (13, 14) governing the fluid flow reduce to the forms

$$4(1-C)\frac{dp}{dz} = (1-C)\frac{\mu_s}{r}\frac{\partial}{\partial r}\left(r\frac{\partial u_f}{\partial r}\right) + CS(u_p - u_f) + \sin\alpha/F, \quad (18)$$

$$4C\frac{dp}{dz} = CS(u_f - u_p) + \sin\alpha/G. \quad (19)$$

Boundary conditions inserted in equations (15, 16), for integrating the above (18-19) equations, reduce to the forms

$$u_f = u_s \quad \text{at} \quad r = R, \quad (20)$$

$$u_f = 0, u_p = \text{finite} \quad \text{at} \quad r = R_1. \quad (21)$$

The non-dimensional flow rate Q can be expressed as

$$Q = \frac{\bar{Q}}{\pi(R_0)^4 q_0 / 8\mu_0} = 4 \int_{R_1}^R r[(1-C)u_f + Cu_p]dr, \quad (22)$$

where

$$\bar{Q} = 2\pi \int_{R_1}^R r[(1-C)\bar{u}_f + C\bar{u}_p]d\bar{r}$$

is the volumetric flow ratio.

The non-dimensional shear stress at a radial distance r is given by

$$\tau_f = \frac{\bar{\tau}_f}{q_0 R_0 / 2} = -\frac{(1-C)\mu_s}{2} \frac{\partial u_f}{\partial r}. \quad (23)$$

3. Integrals

The expressions of velocity for fluid and particle phases in non-dimensional forms are obtained by straight forward integration of equations (18, 19) as follows:

$$u_f = \frac{\log(R_1/r)}{\log(R_1/R)} u_s - \frac{1}{(1-C)\mu_s} \left\{ \frac{dp}{dz} - h \right\} \left[\frac{R^2 \log(R_1/r) - r^2 \log(R_1/R) + R_1^2 \log(r/R)}{\log(R_1/R)} \right], \quad (24)$$

$$u_p = \frac{\log(R_1/r)}{\log(R_1/R)} u_s - \frac{1}{(1-C)\mu_s} \left\{ \frac{dp}{dz} - h \right\} \left[\frac{R^2 \log(R_1/r) - r^2 \log(R_1/R) + R_1^2 \log(r/R)}{\log(R_1/R)} \right]$$

$$+ \frac{4}{CS} [k - C \frac{dp}{dz}], \quad (25)$$

where

$$h = \frac{\sin \alpha}{4H}, k = \frac{\sin \alpha}{4G}, \frac{1}{H} = \frac{1}{F} + \frac{1}{G}.$$

The non-dimensional flow rate from equation (22), is given by

$$Q = (R^2 - R_1^2) \left[\frac{2R^2}{R^2 - R_1^2} - \frac{1}{\log(R/R_1)} \right] \mu_s - \frac{(R^2 - R_1^2)}{(1-C)\mu_s} \left\{ \frac{dp}{dz} - h \right\} \left[(R^2 + R_1^2) - \frac{(R^2 - R_1^2)}{\log(R/R_1)} \right] + \frac{8}{S} (R^2 - R_1^2) \left(k - C \frac{dp}{dz} \right). \quad (26)$$

The expression for pressure gradient $\frac{dp}{dz}$ can be obtained directly from equation (26) as

$$\frac{dp}{dz} = -(1-C)\mu_s I(z), \quad (27)$$

Where

$$I(z) = \frac{Q - (R^2 - R_1^2) [M\mu_s + N\beta + \gamma]}{(R^2 - R_1^2)(N + \xi)}$$

And

$$\beta = \frac{h}{(1-C)\mu_s}, \gamma = \frac{8k}{S}, \xi = \frac{8C(1-C)\mu_s}{S}, M = \frac{2R^2}{R^2 - R_1^2} - \frac{1}{\log(R/R_1)},$$

$$N = (R^2 + R_1^2) - \frac{(R^2 - R_1^2)}{\log(R/R_1)}.$$

From equation (27), the expression for the pressure drop, Δp across the stenosis, may be obtained as

$$\Delta p = \int_0^L \left(-\frac{dp}{dz} \right) dz$$

$$= (1-C)\mu_s \int_0^L I(Z) dz. \quad (28)$$

The resistance to flow (impedance) is given by (using equation (28))

$$\lambda = \frac{\Delta p}{Q} = \frac{1}{Q} (1-C)\mu_s J(z), \quad (29)$$

where

$$\begin{aligned}
 J(z) &= \int_0^L I(z) dz \\
 &= \int_0^d I(z)_{R=1} dz + \int_d^{d+L_0} I(z) dz + \int_{d+L_0}^L I(z)_{R=1} dz.
 \end{aligned}$$

The first and the third integrals in the expression for $J(z)$ are straight forward whereas the analytic evaluation of the second integral is a formidable task. In view of this, one can obtain the final expression for λ as

$$\begin{aligned}
 \lambda &= \frac{1}{Q}(1-C)\mu_s \\
 &\times \frac{Q - (1-R_1^2) \left[\left\{ \frac{2}{1-R_1^2} - \frac{1}{\log(1/R_1)} \right\} u_s + \left\{ (1+R_1^2) - \frac{(1-R_1^2)}{\log(1/R_1)} \beta + \gamma \right\} \right]}{(1+R_1^2) - \frac{(1-R_1^2)}{\log(1/R_1)} + \xi} (L-L_0) \\
 &+ 1/Q(1-C)\mu_s \int_d^{d+L_0} I(z) dz.
 \end{aligned} \tag{30}$$

The expression for wall shear stress, may now be written from equation (23) as

$$\tau_R = \frac{1}{\log(R/R_1)} \left(h - \frac{dp}{dz} \right) \left\{ R \log(R/R_1) - \frac{(R^2 - R_1^2)}{2R} \right\} - \frac{(1-C)\mu_s}{2} \frac{u_s}{R \log(R/R_1)}. \tag{31}$$

The shear stress at the throat of the stenosis can be computed (at $z = d + L_{0/2}, R + \delta = 1, \tau_R = \tau_s$) from equation (31) as

$$\begin{aligned}
 \tau_s &= \frac{1}{\log((1-\delta)/R_1)} \left\{ h - \frac{dp}{dz} \right\} \left\{ (1-\delta) \log((1-\delta)/R_1) - \frac{((1-\delta)^2 - R_1^2)}{2(1-\delta)} \right\} \\
 &\quad - \frac{(1-C)\mu_s}{2} \frac{u_s}{(1-\delta) \log((1-\delta)/R_1)},
 \end{aligned} \tag{32}$$

where

$$\left(\frac{dp}{dz} \right)_0 = -(1-C)\mu_s H(z)$$

is the pressure gradient at the stenotic throat and

$$\begin{aligned}
 H(z) &= \frac{Q - ((1-\delta)^2 - R_1^2) [O u_s + P \beta + \gamma]}{((1-\delta)^2 - R_1^2) (P + \xi)}. \\
 O &= \frac{2(1-\delta)^2}{(1-\delta)^2 - R_1^2} - \frac{1}{\log((1-\delta)/R_1)}, P = ((1-\delta)^2 + R_1^2) - \frac{((1-\delta)^2 - R_1^2)}{\log((1-\delta)/R_1)}.
 \end{aligned}$$

4. Results and Discussions

Analytic expressions for the important flow variables are presented in an earlier section and their variations with several flow parameters are considered here. For this purpose, computer codes have been developed to evaluate the effects of various flow variables as included in equations (24) to (32). The variations of these flow variables with different relevant parameters, like hematocrit C , maximum height attained by the stenosis δ , slip velocity u_s in the stenotic wall, artery inclination α , tapering angle Φ , shape parameter n (≥ 2) and catheter radius R_l in the annular region, are presented graphically for better understanding of the problem. For this computation, we have considered some numerical measures like $\delta=0-0.15$; $u_s=0, 0.05$; $\alpha=0^0$ (horizontal tube), 30^0 (inclined vessel); $C=0-0.6$; $R_l=0.1, 0.2, 0.3$; $\xi(=\tan\Phi)=-1.0, 0, 1.0$ for tapering cases $\Phi <, =, > 0$; $n = 2, 6, 11$; $\bar{a}_0=4\times 10^{-6}\text{m}$; $T=25.5^0\text{C}$ (Srivastava, 2002); $\bar{R}_0=8\times 10^{-5}\text{m}$; $\bar{q}_0=20,000 \text{ kgm}^{-2}\text{s}^{-2}$ (Usha and Prema, 1999); $\bar{\rho}_f=1025 \text{ kgm}^{-3}$; $\bar{\rho}_p=1125 \text{ kgm}^{-3}$ (Chakraborty et al., 2011); $Q=1$ (Sankar and Lee, 2009); $z = d$ to $d + L_0$ and $R_l \leq r \leq R(z)$. In the foregoing analysis, an effort is taken to indicate the variations in flow characteristics due to such parameters.

The present analysis includes

- (i) the model of Chakraborty et al. (2011) when $R_l = 0, \Phi = 0$;
- (ii) the analysis of Srivastava (2002) for $u_s = 0, \alpha = 0$ and $R_l = 0, \Phi = 0$;
- (iii) the Srivastava and Rastogi (2010) model when $u_s=0, \alpha=0$ and $\Phi=0$;
- (iv) the tapered or non-tapering ($\Phi \geq 0$) models with slip ($u_s > 0$) and zero slip ($u_s = 0$) for inclined ($\alpha > 0$) and horizontal ($\alpha = 0$) vessels, with or without stenosis ($\delta \geq 0$);
- (v) the catheterized tapering or non-tapering ($\Phi \geq 0$) models with slip or no-slip ($u_s \geq 0$) cases for inclined or horizontal ($\alpha \geq 0$) tube, with or without constriction ($\delta \geq 0$), as its special cases .

The velocity, in equations (24-25) is a function of several flow parameters and co-ordinates.

The variations of axial velocity u_f versus the radial distance r for different values of R_l and α are shown in Figures (3-4). Figures (5-6) shows the variation of axial velocity u_f versus radial distance r for different values of slip velocity u_s and hematocrit C . The variation of the pressure gradient, using equation (27), with the axial distance, for different values of catheter radius R_l , inclination α , slip velocity u_s and hematocrit C are depicted in Figures (7-10).

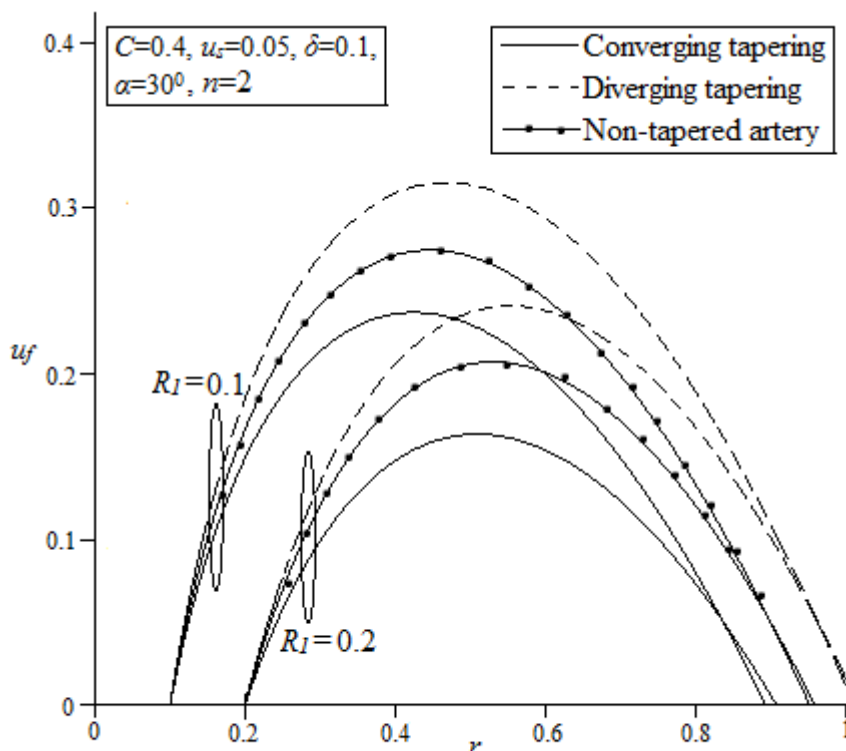


Figure 3. Variation of axial velocity u_f with radial distance r for different values of R_I

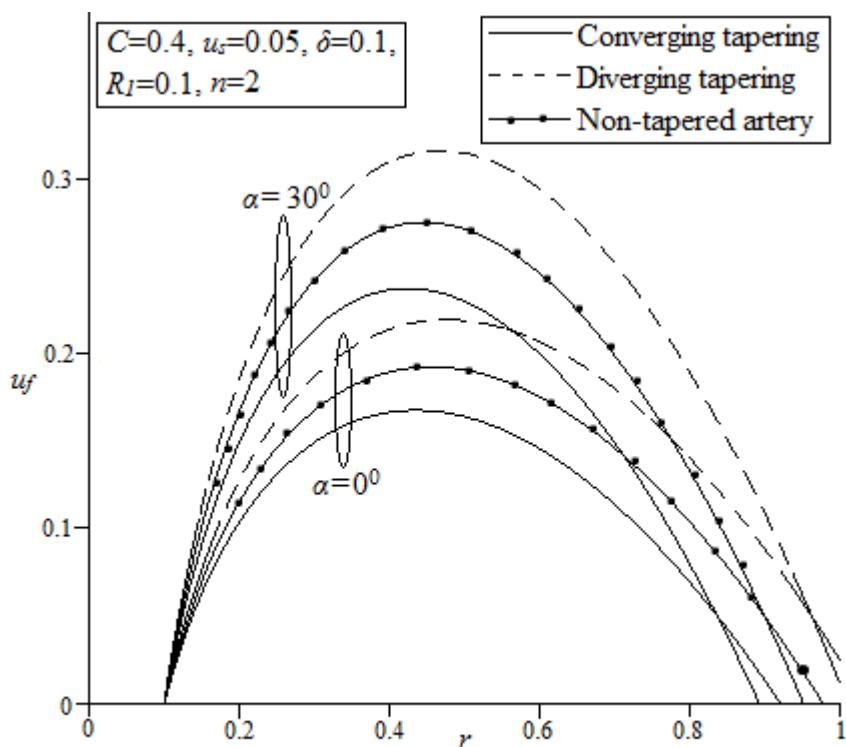


Figure 4. Variation of axial velocity u_f with radial distance r for different values of α

In this unidirectional flow, the profiles for the axial velocity versus the radial distance through the annular region ($R_1 \leq r \leq R$), clearly indicate a deviation from the usual parabolic profiles. As the radial co-ordinate r increases in the full scale from R_1 to R . The velocity increases rapidly to a greater value, wherefrom, it gradually decreases to a lower value at or near the vessel wall. It is observed from Figure 3 that as the catheter radius R_I increases, velocity

decreases. As expected, the velocity decreases with the rise in catheter radius (Figure 3) but it is found that the velocity increases, with the increase in inclination (α) of the artery (Figure 4).

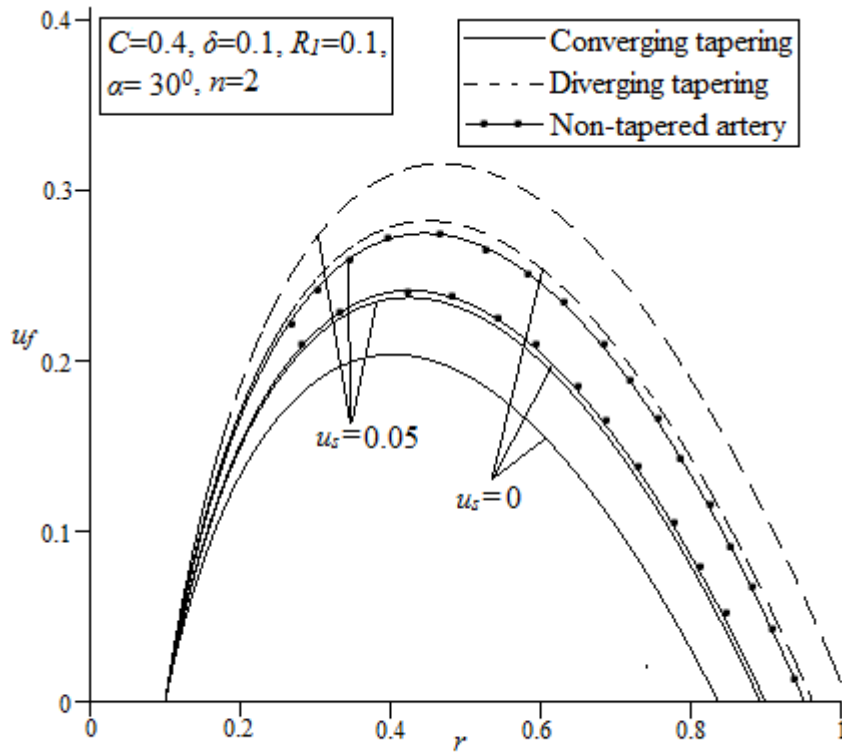


Figure 5. Variation of axial velocity u_f with radial distance r for different values of u_s

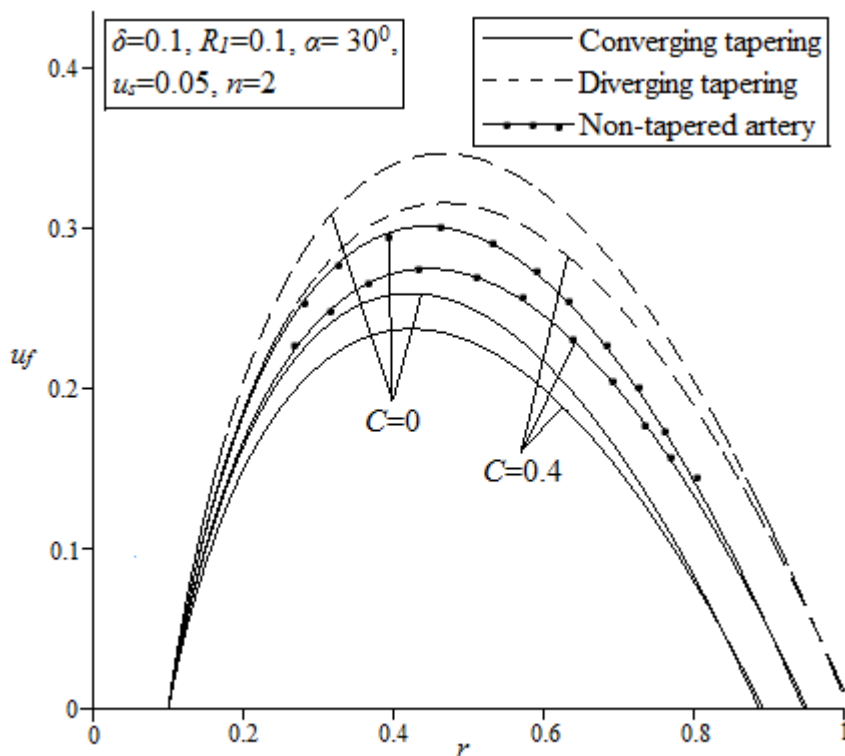


Figure 6. Variation of axial velocity u_f with radial distance r for different values of C

The velocity increases with slip employed at the stenotic wall. Its values are higher for the flows with slip ($u_s > 0$) than those with no slip (Figure 5). The profiles indicate that an increase in hematocrit C decreases the velocity of the blood (Figure 6). The magnitude of the velocity shows the lowest for converging tapering tube, higher in case of a non-tapered artery and highest for the diverging tapering vessel.

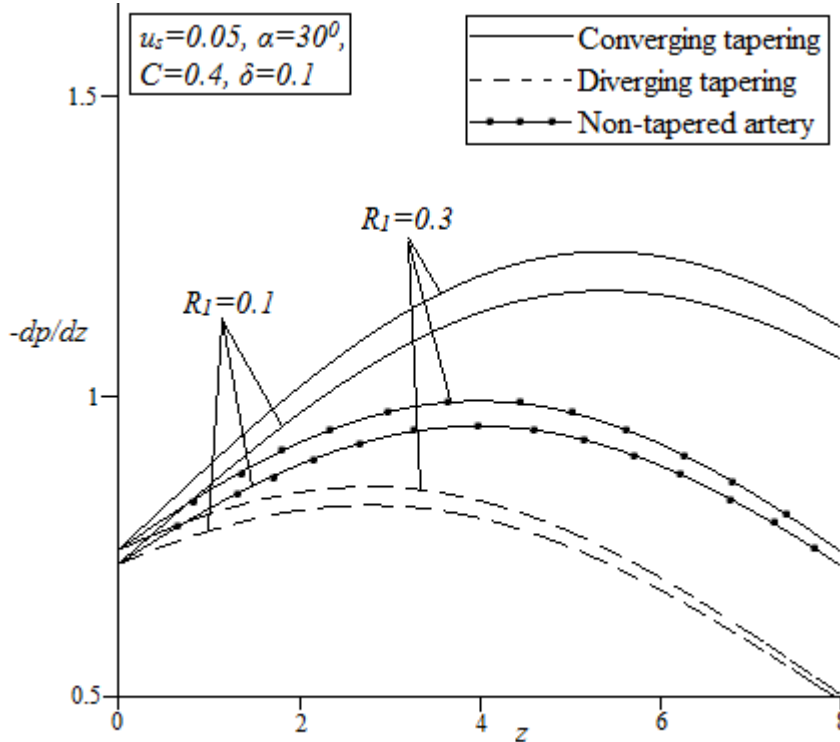


Figure 7. Variation of pressure gradient ($-dp/dz$) with axial distance z for different values of R_I

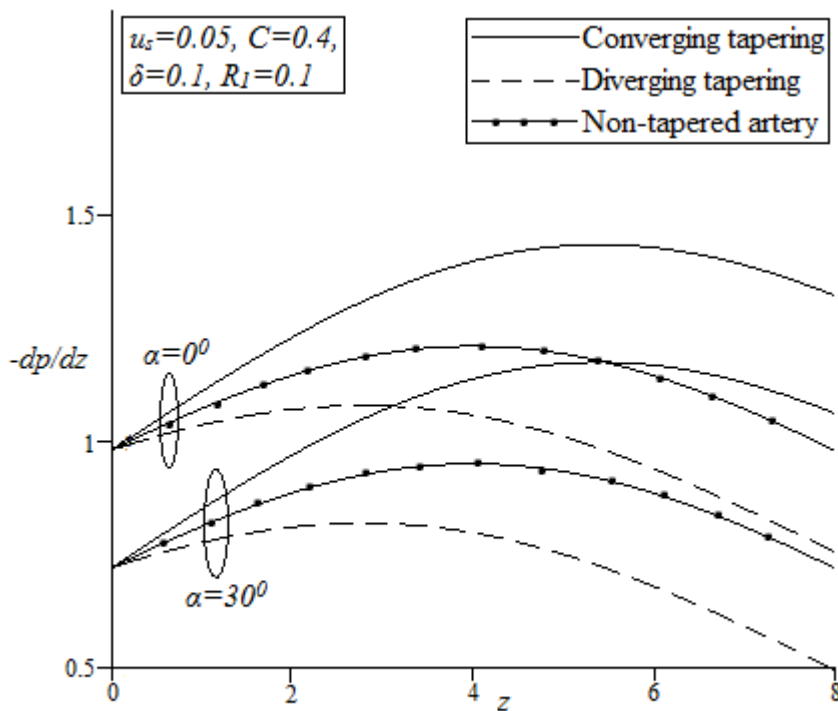


Figure 8. Variation of pressure gradient ($-dp/dz$) with axial distance z for different values of α

It could be noticed that the pressure gradient increases from a lower magnitude at one end of the stenosis, and gradually attains the maximum at the stenosis throat and there from, it decreases to almost the same lower value. However pressure gradient attains the highest value at the throat of a stenosis and the lower value at the two ends of a stenosis.

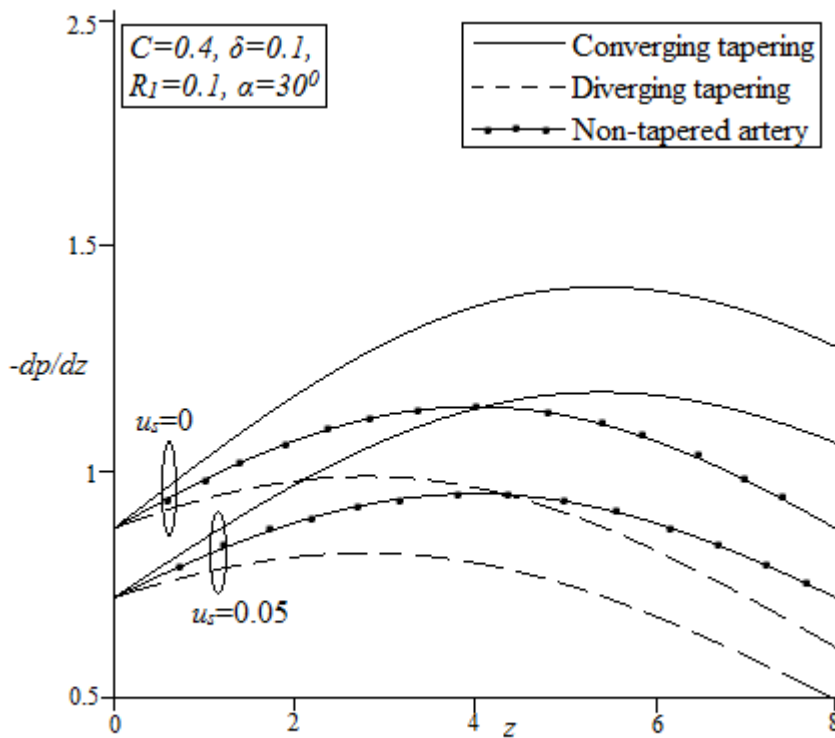


Figure 9. Variation of pressure gradient ($-dp/dz$) with axial distance z for different values of u_s

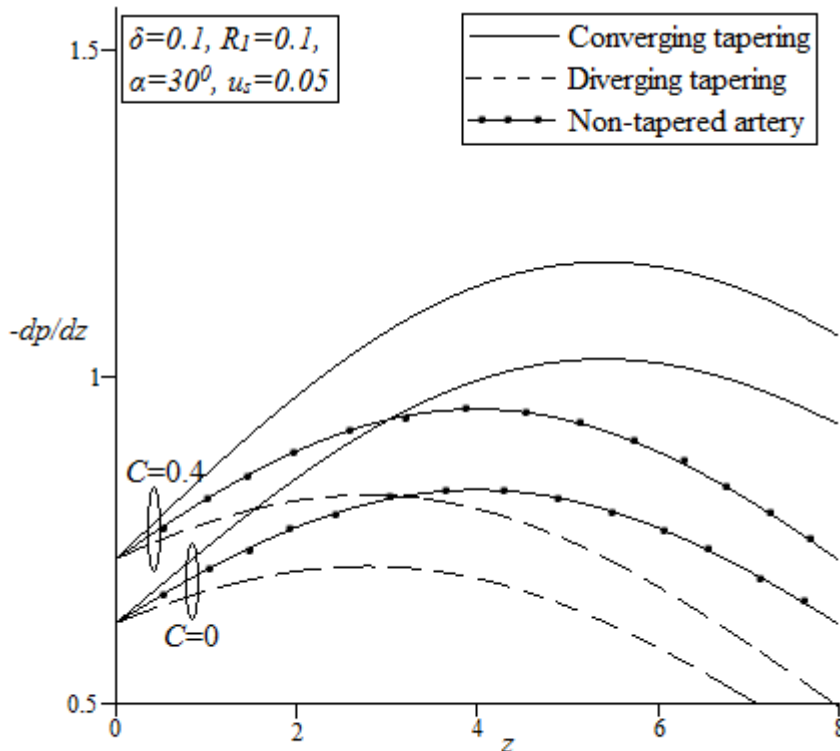


Figure 10. Variation of pressure gradient ($-dp/dz$) with axial distance z for different values of C

As the catheter radius R_I increases the pressure gradient also increases (Figure 7), but the pressure gradient decreases with the increase in inclination (α) of the artery (Figure 8). It may be noted that in all such variations, pressure gradient decreases with the employment of a velocity slip (u_s) at the vessel wall (Figure 9) but increases with increase with the hematocrit C (Figure 10). Also for a diverging tapering with taper angle $\Phi > 0$, the pressure gradient is lower as compare to converging tapering ($\Phi < 0$) and without tapering ($\Phi = 0$).

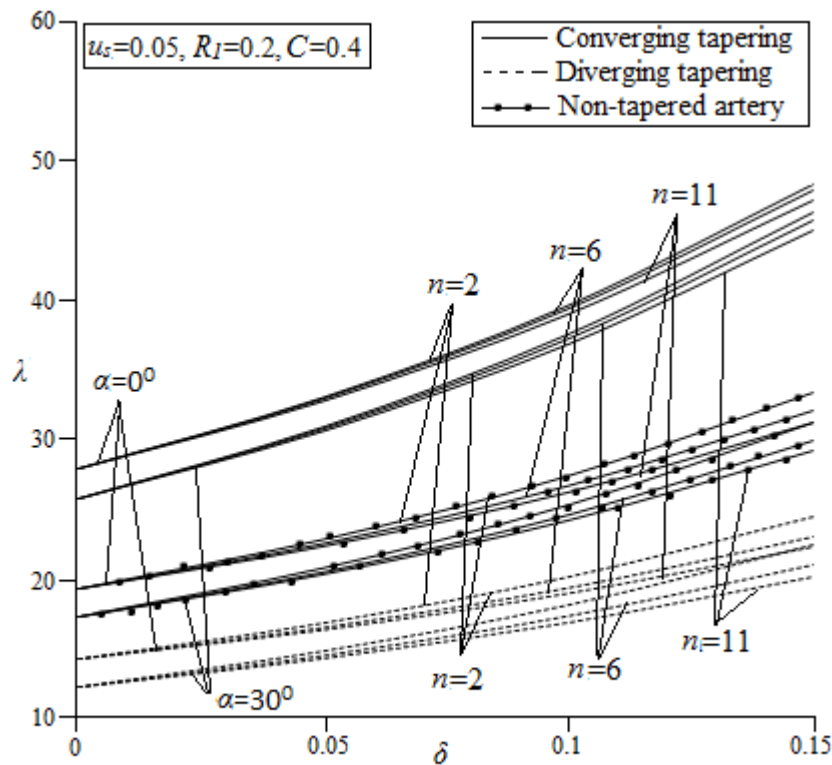


Figure 11. Variation of resistance to flow λ with δ for different values of n and α

The variation of the resistance to the flow λ versus the maximum height of the stenosis δ for different magnitudes of the parameters n , Φ , α and for different values of C , n and Φ , are shown in Figures 11-12. The variation of impedance λ with hematocrit parameter C for different values of n , u_s and Φ , is presented in Figure 13 and, Figure 14 shows the profile for λ versus δ for variation in R_I , n and Φ . In Figure 15, the profile of the wall shear stress distribution τ_R against the axial distance z for variation of n , R_I and Φ , is drawn. Figure 16 shows the variation of the shear stress at the stenotic throat versus stenosis height δ for different values of C and u_s . In Figure 17 variation of τ_s with R_I for different values of u_s and δ is shown.

In this catheterized tapering inclined artery region, it could be noticed that the resistance (impedance) to flow λ increases with the maximum stenosis height δ and, decreases with the rise in both the shape parameter n and inclination α of the artery (Figure 11), but the impedance λ increases as the hematocrit C increases (Figure 12). In Figure 13, it is clearly noticed that the resistance λ , experienced by the streaming fluid over the whole arterial segment in the annular region increases with the hematocrit C but decreases with the slip velocity u_s attained by the fluid at the constricted wall and shape parameter $n(\geq 2)$ of the stenosis. It is seen in Figure 14 that as catheter radius R_I increases, impedance (λ) to flow increases. However, resistance increases with stenosis height δ but decreases with the rise in

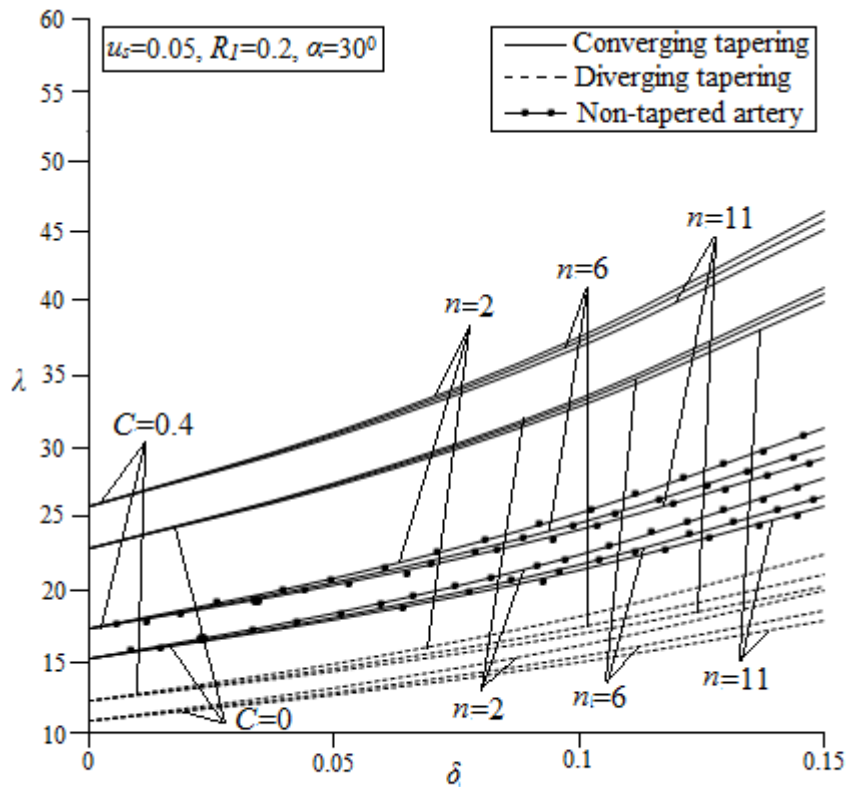


Figure 12. Variation of resistance to flow λ with δ for different values of n and C

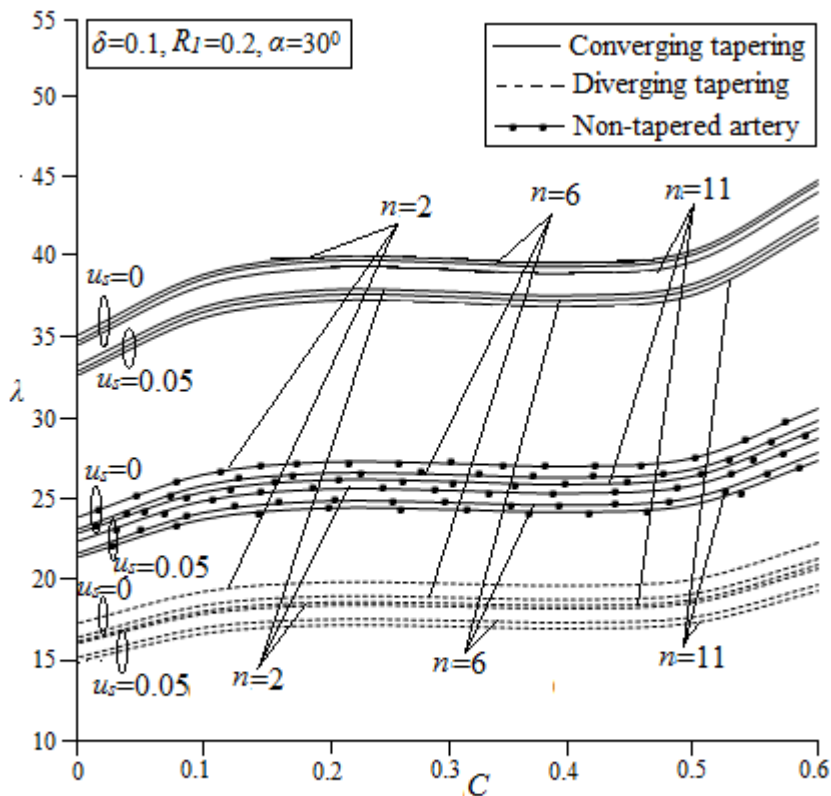


Figure 13. Variation of λ with hematocrit C for different values of n and u_s

shape parameter n . For any given value of stenosis height δ as the hematocrit increases from 0 to 0.1, resistance to flow increases steeply, the increment is relatively slower from $C = 0.1$ to 0.5 and again, it goes on increasing rapidly from $C = 0.5$ to 0.6 (Figure 13). However, an

employment of velocity slip at vessel wall, decreases the resistance if the other parameters are kept constant. The behaviour of resistance in tapering region ($\Phi >, =, < 0$) of the constricted artery in this annular flow is reflected as, $|\lambda|_{\text{diverging tapering}} < |\lambda|_{\text{non-tapering}} < |\lambda|_{\text{converging tapering}}$.

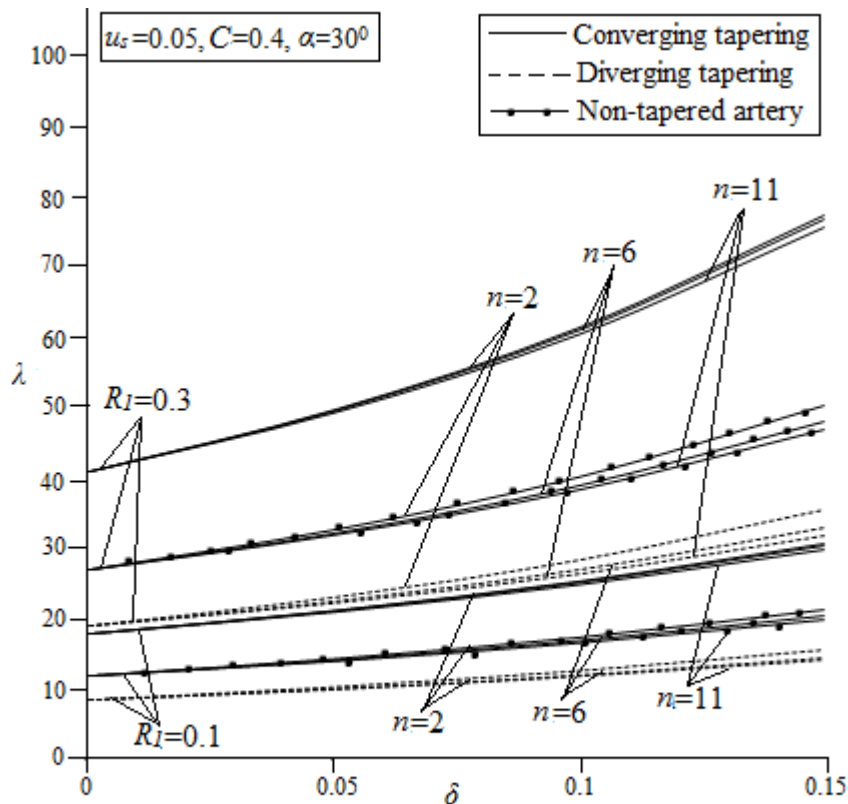


Figure 14. Variation of resistance to flow λ with δ for different values of n and R_I

The impedance (λ) to the flow is influenced by the shape parameter as its magnitude is seen to be lower in asymmetric stenosis ($n > 2$) than that in axi-symmetric stenosis ($n = 2$). As expected, resistance λ increases with the rise in catheter radius but it decreases, as we consider a horizontal artery ($\alpha = 0^\circ$) to an inclined tube ($\alpha > 0^\circ$). The consideration $\bar{\delta}/\bar{R}_0 = \delta \ll 1$ (for mild stenosis case) could make this analysis useful only in the formative (early) stage of a stenosis. The range of the parameter δ is restricted upto 0.15 (i.e., 28% of area reduction), as beyond this quantity, flow separation may happen for even very low magnitude Reynolds number (Young, 1968). Numerical results further reveal that the resistance assumes an asymptotic magnitude at about $n=11$, that in turn implies that no significant change in the flow would occur beyond this magnitude of shape parameter n . This behaviour in λ conforms to the results obtained by Srivastava (2002), Srivastava and Rastogi (2010), and, Chakraborty et al. (2011).

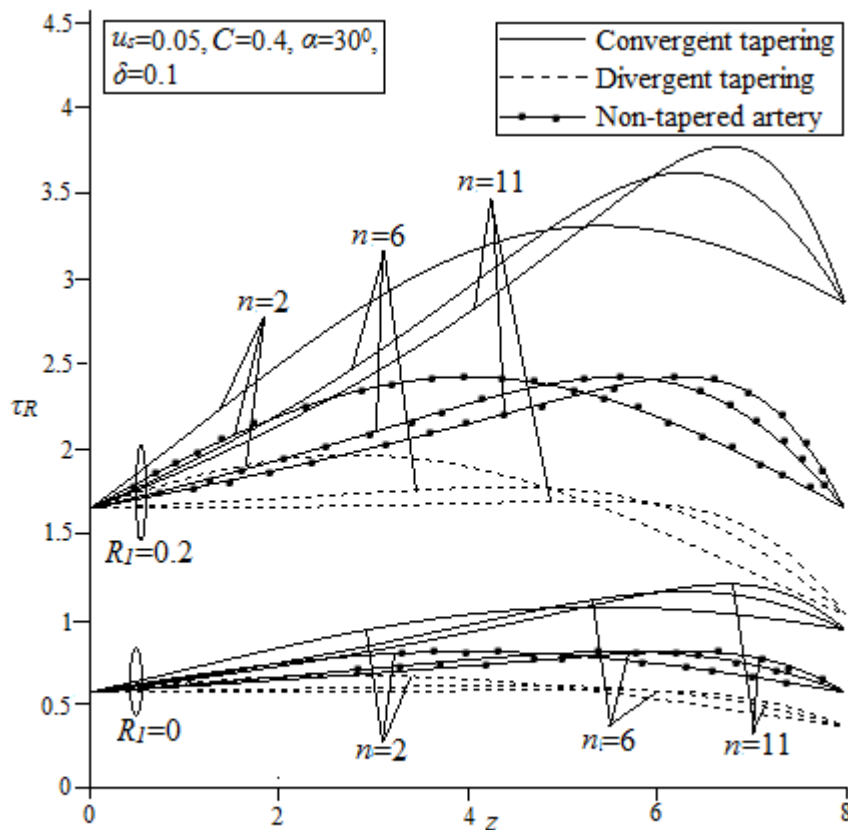


Figure 15. Variation of wall shear stress with axial distance for different values of n and R_I

The wall shear stress τ_R in this annular stenotic region ($d \leq z \leq d+L_0$) increases rapidly from its approached value (initiation point) at $z=d$ in the upstream of the stenotic throat and attains its maximum magnitude at the throat, wherefrom it decreases rapidly to a lower magnitude at the termination (end point) of the constricted region at $z = d+L_0$ (Figure 15). The wall shear stress τ_R decreases with increasing shape parameter n in the upstream of the throat but this behaviour reverses in the downstream. As the catheter radius R_I increases in the constricted annular region (with other parameters keeping fixed), τ_R decreases from a higher value to a lower one.

It is also observed that wall shear stress at any axial distance increases with tapering angle Φ (from $\Phi > 0$, $\Phi = 0$, $\Phi < 0$) of the inclined tube as follows τ_R (divergent tapering tube) $<$ τ_R (non-tapering tube) $<$ τ_R (converging tapering tube).

It could be observed from Figures 16 and 17 that the wall shear stress at the peak of the stenosis τ_s , increases with both stenosis height δ and hematocrit C , for any given value of the angle of inclination of the artery (α) and catheter radius (R_I). However, τ_s decreases with velocity slip u_s , at the stenotic wall in the constricted annular region. As the catheter radius R_I increases for given magnitudes of C and α , τ_s increases as δ increases but it decreases with velocity slip at the wall.

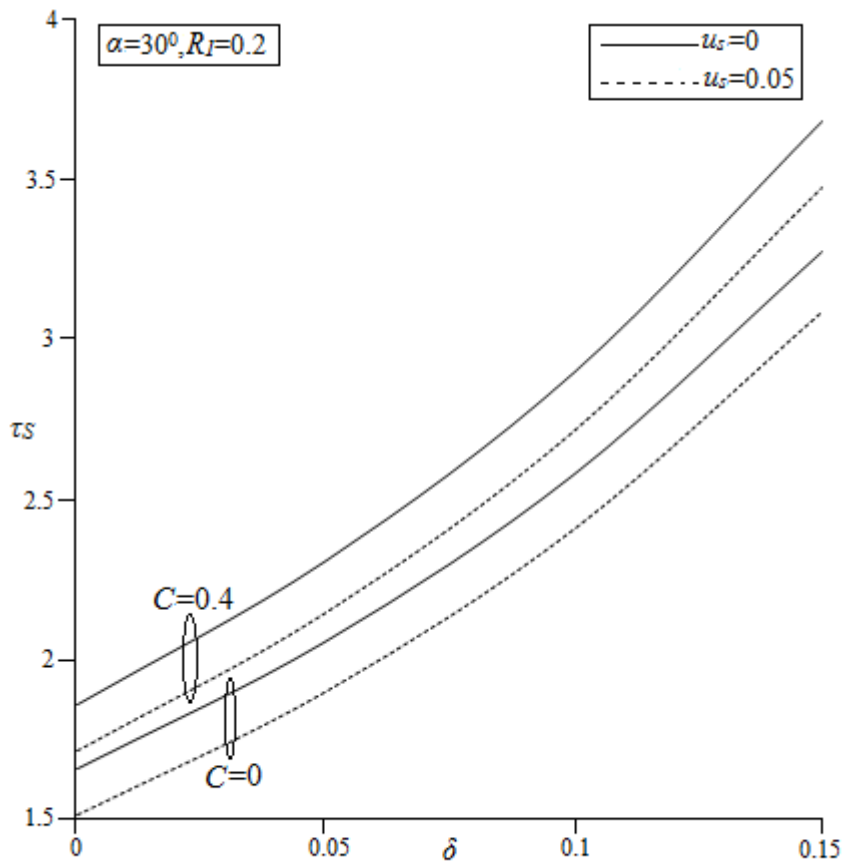


Figure 16. Variation of τ_S with δ for different values of C and u_s

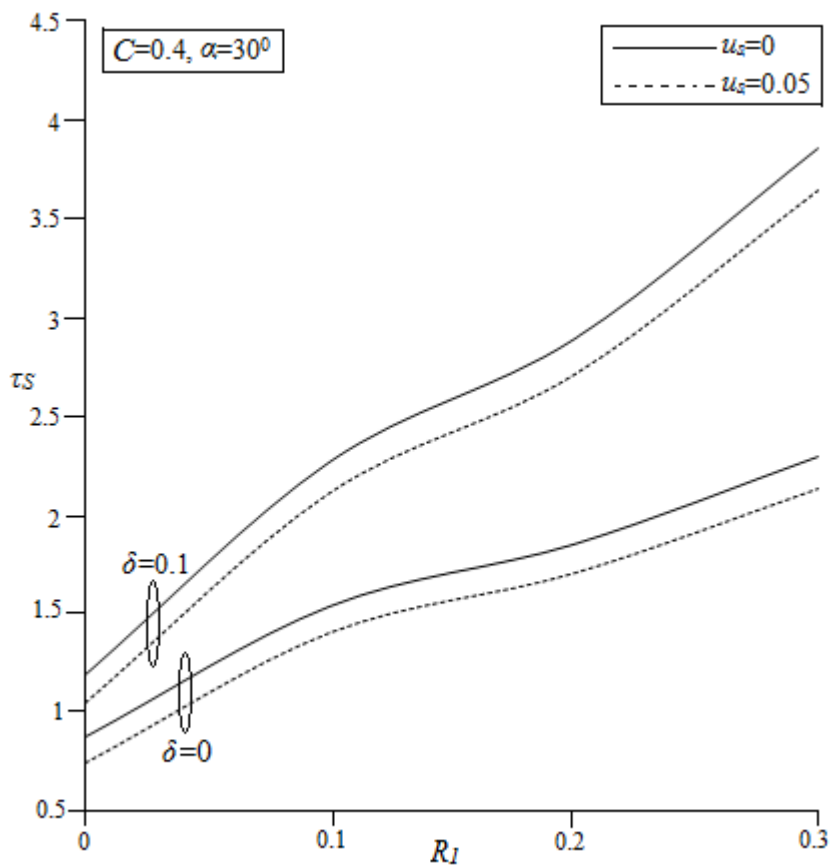


Figure 17. Variation of τ_S with R_I for different values of u_s and δ

5. Conclusion

To account for the combined influence of several flow parameters like slip velocity, hematocrit, catheter radius, tapering geometry, shape parameter and inclination of the vessel a two phase annular model, on assuming that blood is represented by a suspension of erythrocytes in plasma, has been considered. The annular region is spaced within an inclined, tapering, constricted (-asymmetric stenosis) wall and a co-axial catheter. Analytical expressions of the flow variables are obtained and the variations of the important flow characteristics such as, velocity, pressure gradient, resistance (impedance) to flow and wall shear stress, have been included.

The flow characteristics (viz., resistance to flow, wall shear stress in the stenotic region and shear stress at the throat of the constriction) increase with hematocrit, stenosis height and catheter radius. It may be interesting to observe that the resistance to the flow decreases with the inclination of the tapering vessel. However, all the three flow characteristics decrease with velocity slip at the stenotic wall. Both the resistance to the flow and the wall shear stress are seen to be higher in the case of axially symmetric stenosis than those in case of axially non-symmetric ones. It is also exhibited that both these flow variables attain the lower magnitude in a diverging tapering region than that in the non-tapering tube which value is lower than that obtained in a converging tapering vessel.

The present analysis includes the models of Srivastava, Srivastava and Rastogi and Chakraborty et al., uniform, tapering and catheterized models for inclined or horizontal vessels with velocity slip or zero slip at stenotic wall, as its special cases.

It is already reported that arterial stenosis or atherosclerosis is a common and wide spread disease that may severally influence human health in general and cardiovascular system in particular. In the present analysis, a mild stenosis formation has been dealt with. However, its gradual growth from mild to moderate stage and moderate to severe forms at certain locations eg. , carotid, bifurcations, coronary arteries, distal to abdominal aorta etc. , could lead to serious complications inside the body and several health hazards, like reduction in blood supply, cut off in nutrition supply, stroke, thrombosis, renal problems, circulatory disorders etc. Theoretical models can throw some insight into the complicated situations and in turn, it could suggest some measures in regulating the normal blood flow and nutrition supply to each and every body organ, tissue, cell etc.

In this analysis, it is observed that a velocity slip condition employed at the constricted tapering vessel wall may accelerate the flow of the one hand and, retard the resistance to flow and wall shear stress on the other. Thus, by employing an appropriate velocity slip, damages to the diseased vessel wall could be reduced and bore of the blood vessel could be enlarged. It is therefore necessary to determine an appropriate velocity slip in accordance with the hematocrit, stenosis size, artery radius and other physiological situations. Theoretical analysis could be improved by considering a two-dimensional, pulsatile, two-layered annular model with employing slips in both radial and axial directions and, with permeability of the arterial wall. Such models could be used as a device in the initiation of atherosclerosis and also in the treatment modalities of cardiovascular complications, cardiac arrest, haematological, stroke, thrombosis, renal and sickle cell diseases and other arterial disorders.

Acknowledgement

This research work is supported by the UGC, New Delhi, India (MRP Grant Reference No. : AU:MS:UGC-MRPF: 2011:01). Authors are also grateful to the Editor-in-Chief Prof. A. M. Haghghi and the Reviewer, for their valuable comments.

REFERENCES

- Biswas, D. and Chakraborty, U.S. (2009). Pulsatile flow of blood in a constricted artery with body acceleration, *Appl. Appl. Math.* , Vol. 4, pp 329-342.
- Biswas, D. and Paul, M. (2012). Mathematical Modelling of Blood Flow Through Inclined Tapered Artery With Stenosis, *AUJST*, Vol. 10(II), pp 10-18.
- Charm, S.E. and Kurland, G.S. (1974). *Blood flow and microcirculation*, John Wiley, New York.
- Chakraborty, U.S. , Biswas, D. and Paul, M. (2011). Suspension model blood flow through an inclined tube with an axially non-symmetrical stenosis, *Korea Australia Rheology Journal*, Vol. 23(1), pp 25-32.
- Fung, Y.C. (1981). *Biomechanics: Mechanical Properties of Living Tissues*, Springer-Verlag, New York.
- Guyton, A.C. (1970). *Text Book of Medical Physiology*, W.B. Saunders, Philadelphia.
- Haynes, R.H. (1960). Physical basis on dependence of blood viscosity on tube radius, *Am. J. Physiol.*, Vol. 198, pp 1193-1205.
- Ku, D. (1997). Blood flow in arteries, *Ann. Rev. Fluid Mech.* , Vol. 29, pp 399-434.
- Lightfoot, E.N. (1974). *Transport Phenomenon in Living Systems*, New York, Wiley.
- Maruti Prasad, K. and Radhakrishnamcharya, G. (2008). Flow of herschel-bulkley fluid through an inclined tube of non-uniform cross-section with multiple stenoses, *Arch. Mech.*, Vol. 60(2), pp 161-172.
- MacDonald, D.A. (1979). On steady flow through modelled vascular stenosis, *J. Biomechanics*, Vol. 12, pp 13-20.
- Mekheimer, K.S. and Kothari, M.A.E. (2008). The micropolar fluid model for blood flow through a tapered artery with a stenosis, *Acta Mech. Sin.* , Vol. 24, pp 637-644.
- Mekheimer, K.S. and Kothari, M.A.E. (2010). Suspension model for blood flow through arterial catheterization, *Chem. Eng. Comm.* , Vol. 197, pp 1195-1214.
- Merril, E.W. and Pelletier, G.A. (1967). Viscosity of human blood: transition from Newtonian to non-Newtonian, *J. Appl. Physiol.* , Vol 23, pp 178-182.
- Sankar, D.S. and Lee, U. (2009). Mathematical modelling of pulsatile flow of non-Newtonian fluid in stenosed arteries, *Commun. Nonlinear Sci. Numer. Simulat.* , Vol. 14, pp 2971-2981.
- Srivastava, V.P. (1995). Particle-fluid suspension model of blood flow through stenotic vessels with applications, *Int. J. Biomed. Compt.* , Vol. 38, pp 141-154.
- Srivastava, V.P. (2002). Particle suspension blood flow through stenotic arteries: effects of hematocrit and stenosis shape, *Indian J. Pure Appl. Math.* , Vol. 33, pp 1353-1360.
- Srivastava, V.P. and Rastogi, R. (2010). Blood flow through a stenosed catheterized artery: Effects of hematocrit and stenosis shape, *Comput. Math. Appl.* , Vol. 59, pp 1377-1385.
- Srivastava, L.M. and Srivastava, V.P. (1983). On Two-phase Model of Pulsatile Blood Flow with Entrance Effects, *Biorheology*, Vol. 20, pp 761-777.
- Srivastava, V.P. , Rastogi, R. and Vishnoi, R. (2010). A two-layered suspension blood flow through an overlapping stenosis, *Comput. Math. Appl.* , Vol 60(3), 432-441.

- Sud, V.K. and Sekhon, G.S. (1985). Arterial flow under Periodic body acceleration, *Bull. Math. Biol.* , Vol 47(1), pp 35-52.
- Usha, R. and Prema, K. (1999). Pulsatile flow of particle-fluid suspension model of blood under periodic body acceleration, *Z. Angew. Math. Phys.* , Vol. 50, pp 175-192.
- Womersley, J.R. (1955). Method for the calculation of Velocity rate of Flow and Viscous Drag in Arteries when pressure gradient is known, *J. Physiol.* , Vol. 127, pp 533-563.
- Young, D.F. (1968). Effects of Time-Dependent Stenosis on Flow Through a Tube, *J. Eng. Ind. Trans. ASME.* , Vol. 90, pp 248-254.